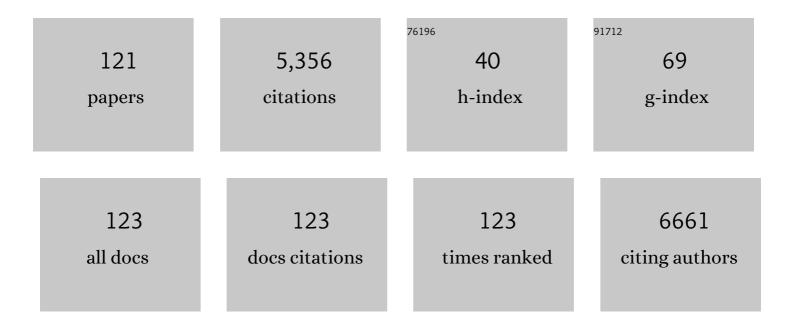
## List of Publications by Year in descending order

Source: https://exaly.com/author-pdf/9063995/publications.pdf

Version: 2024-02-01



#	Article	IF	CITATIONS
1	MOFâ€Derived Hollow CoS Decorated with CeO <sub><i>x</i></sub> Nanoparticles for Boosting Oxygen Evolution Reaction Electrocatalysis. Angewandte Chemie - International Edition, 2018, 57, 8654-8658.	7.2	369
2	Ce-Doped NiFe-Layered Double Hydroxide Ultrathin Nanosheets/Nanocarbon Hierarchical Nanocomposite as an Efficient Oxygen Evolution Catalyst. ACS Applied Materials & Interfaces, 2018, 10, 6336-6345.	4.0	276
3	A ratiometric fluorescent nanoprobe based on terbium functionalized carbon dots for highly sensitive detection of an anthrax biomarker. Chemical Communications, 2015, 51, 5036-5039.	2.2	191
4	3D nitrogen-doped framework carbon for high-performance potassium ion hybrid capacitor. Energy Storage Materials, 2019, 23, 522-529.	9.5	190
5	Optimized Metal Chalcogenides for Boosting Water Splitting. Advanced Science, 2020, 7, 1903070.	5.6	190
6	A Stimuliâ€Responsive Smart Lanthanide Nanocomposite for Multidimensional Optical Recording and Encryption. Angewandte Chemie - International Edition, 2017, 56, 2689-2693.	7.2	181
7	CeO <sub><i>x</i></sub> -Decorated NiFe-Layered Double Hydroxide for Efficient Alkaline Hydrogen Evolution by Oxygen Vacancy Engineering. ACS Applied Materials & Interfaces, 2018, 10, 35145-35153.	4.0	156
8	Metal–organic framework derived CoTe <sub>2</sub> encapsulated in nitrogen-doped carbon nanotube frameworks: a high-efficiency bifunctional electrocatalyst for overall water splitting. Journal of Materials Chemistry A, 2018, 6, 3684-3691.	5.2	153
9	Hollow bimetallic cobalt-based selenide polyhedrons derived from metal–organic framework: an efficient bifunctional electrocatalyst for overall water splitting. Journal of Materials Chemistry A, 2017, 5, 17982-17989.	5.2	139
10	A Stimuliâ€Responsive Smart Lanthanide Nanocomposite for Multidimensional Optical Recording and Encryption. Angewandte Chemie, 2017, 129, 2733-2737.	1.6	132
11	Fabrication of layered double hydroxide microcapsules mediated by cerium doping in metal–organic frameworks for boosting water splitting. Energy and Environmental Science, 2020, 13, 2949-2956.	15.6	126
12	Plant Sunscreen and Co(II)/(III) Porphyrins for UVâ€Resistant and Thermally Stable Perovskite Solar Cells: From Natural to Artificial. Advanced Materials, 2018, 30, e1800568.	11.1	114
13	Terbium Functionalized Micelle Nanoprobe for Ratiometric Fluorescence Detection of Anthrax Spore Biomarker. Analytical Chemistry, 2018, 90, 3600-3607.	3.2	110
14	A new Ce-doped MgAl-LDH@Au nanocatalyst for highly efficient reductive degradation of organic contaminants. Journal of Materials Chemistry A, 2017, 5, 6716-6724.	5.2	108
15	Intramolecular Electric Field Construction in Metal Phthalocyanine as Dopantâ€Free Hole Transporting Material for Stable Perovskite Solar Cells with >21 % Efficiency. Angewandte Chemie - International Edition, 2021, 60, 6294-6299.	7.2	101
16	Efficient Grain Boundary Suture by Low-Cost Tetra-ammonium Zinc Phthalocyanine for Stable Perovskite Solar Cells with Expanded Photoresponse. Journal of the American Chemical Society, 2018, 140, 11577-11580.	6.6	95
17	CeO <i><sub>x</sub></i> -Decorated Hierarchical NiCo <sub>2</sub> S <sub>4</sub> Hollow Nanotubes Arrays for Enhanced Oxygen Evolution Reaction Electrocatalysis. ACS Applied Materials & Interfaces, 2019, 11, 39841-39847.	4.0	95
18	MOFâ€Đerived Hollow CoS Decorated with CeO <sub><i>x</i></sub> Nanoparticles for Boosting Oxygen Evolution Reaction Electrocatalysis. Angewandte Chemie, 2018, 130, 8790-8794.	1.6	84

#	Article	IF	CITATIONS
19	A core–shell metal–organic-framework (MOF)-based smart nanocomposite for efficient NIR/H <sub>2</sub> O <sub>2</sub> -responsive photodynamic therapy against hypoxic tumor cells. Journal of Materials Chemistry B, 2017, 5, 2390-2394.	2.9	83
20	A new multicomponent CDs/Ag@Mg–Al–Ce-LDH nanocatalyst for highly efficient degradation of organic water pollutants. Journal of Materials Chemistry A, 2018, 6, 4515-4524.	5.2	75
21	Ion regulation of ionic liquid electrolytes for supercapacitors. Energy and Environmental Science, 2021, 14, 2859-2882.	15.6	71
22	Facile synthesis of Co and Ce dual-doped Ni3S2 nanosheets on Ni foam for enhanced oxygen evolution reaction. Nano Research, 2020, 13, 2130-2135.	5.8	70
23	A novel peptide-based fluorescence chemosensor for selective imaging of hydrogen sulfide both in living cells and zebrafish. Biosensors and Bioelectronics, 2017, 92, 602-609.	5.3	66
24	Perfection of Perovskite Grain Boundary Passivation by Euâ€Porphyrin Complex for Overallâ€Stable Perovskite Solar Cells. Advanced Science, 2019, 6, 1802040.	5.6	65
25	Facile fabrication of color-tunable and white light emitting nano-composite films based on layered rare-earth hydroxides. Journal of Materials Chemistry C, 2015, 3, 2326-2333.	2.7	64
26	NIR light/H <sub>2</sub> O <sub>2</sub> -triggered nanocomposites for a highly efficient and selective synergistic photodynamic and photothermal therapy against hypoxic tumor cells. Chemical Communications, 2016, 52, 7939-7942.	2.2	64
27	A peptide-based fluorescent chemosensor for multianalyte detection. Biosensors and Bioelectronics, 2015, 72, 80-86.	5.3	63
28	Composition-Engineered Metal–Organic Framework-Based Microneedles for Glucose-Mediated Transdermal Insulin Delivery. ACS Applied Materials & Interfaces, 2020, 12, 13613-13621.	4.0	61
29	Functionalized Eu(III)-Based Nanoscale Metal–Organic Framework To Achieve Near-IR-Triggered and -Targeted Two-Photon Absorption Photodynamic Therapy. Inorganic Chemistry, 2018, 57, 300-310.	1.9	55
30	Stringing MOF-derived nanocages: a strategy for the enhanced oxygen evolution reaction. Journal of Materials Chemistry A, 2019, 7, 8284-8291.	5.2	53
31	Fixedâ€Component Lanthanideâ€Hybridâ€Fabricated Fullâ€Color Photoluminescent Films as Vapoluminescent Sensors. Chemistry - A European Journal, 2013, 19, 4556-4562.	1.7	51
32	Hybrid Metal–Organic-Framework/Inorganic Nanocatalyst toward Highly Efficient Discoloration of Organic Dyes in Aqueous Medium. Inorganic Chemistry, 2018, 57, 13270-13278.	1.9	51
33	A paper-based lanthanide smart device for acid–base vapour detection, anti-counterfeiting and logic operations. Inorganic Chemistry Frontiers, 2016, 3, 1014-1020.	3.0	50
34	Cerium-Oxide-Modified Anodes for Efficient and UV-Stable ZnO-Based Perovskite Solar Cells. ACS Applied Materials & Interfaces, 2019, 11, 13273-13278.	4.0	50
35	One dimensional graphene nanoscroll-wrapped MnO nanoparticles for high-performance lithium ion hybrid capacitors. Journal of Materials Chemistry A, 2021, 9, 6352-6360.	5.2	50
36	Gadolinium functionalized carbon dots for fluorescence/magnetic resonance dual-modality imaging of mesenchymal stem cells. Journal of Materials Chemistry B, 2016, 4, 7472-7480.	2.9	46

#	Article	IF	CITATIONS
37	Self-Assembled Upconversion Nanoparticle Clusters for NIR-controlled Drug Release and Synergistic Therapy after Conjugation with Gold Nanoparticles. Inorganic Chemistry, 2017, 56, 5295-5304.	1.9	45
38	Hollow CeO <sub>x</sub> /CoP Heterostructures Using Twoâ€dimensional Coâ^'MOF as Template for Efficient and Stable Electrocatalytic Water Splitting. ChemNanoMat, 2020, 6, 1119-1126.	1.5	45
39	Dramatically Enhanced Luminescence of Layered Terbium Hydroxides as Induced by the Synergistic Effect of Gd <sup>3+</sup> and Organic Sensitizers. Journal of Physical Chemistry C, 2014, 118, 14511-14520.	1.5	44
40	Highly Stable Perovskite Quantum Dots Modified by Europium Complex for Dual-Responsive Optical Encoding. ACS Nano, 2021, 15, 6266-6275.	7.3	44
41	Encapsulation and Regeneration of Perovskite Film by in Situ Forming Cobalt Porphyrin Polymer for Efficient Photovoltaics. CCS Chemistry, 2020, 2, 488-494.	4.6	41
42	A novel peptide-based fluorescent chemosensor for measuring zinc ions using different excitation wavelengths and application in live cell imaging. Journal of Materials Chemistry B, 2015, 3, 3617-3624.	2.9	40
43	Construction of Supercapacitorâ€Based Ionic Diodes with Adjustable Bias Directions by Using Poly(ionic) Tj ETQq	1 1 0.784 11.1	314 rgBT /0 40
44	Novel three-dimensional network generated from the reaction of Eu(NO3)3 with an amide type tripodal ligand. Dalton Transactions RSC, 2002, , 832.	2.3	39
45	Fluorescence "on–off–on―peptide-based chemosensor for the selective detection of Cu <sup>2+</sup> and S <sup>2â''</sup> and its application in living cell bioimaging. Dalton Transactions, 2016, 45, 16246-16254.	1.6	36
46	A Smart Photosensitizer–Cerium Oxide Nanoprobe for Highly Selective and Efficient Photodynamic Therapy. Inorganic Chemistry, 2019, 58, 7295-7302.	1.9	36
47	Smart All-in-One Thermometer-Heater Nanoprobe Based on Postsynthetical Functionalization of a Eu(III)-Metal–Organic Framework. Analytical Chemistry, 2019, 91, 5225-5234.	3.2	36
48	Copper-copper iodide hybrid nanostructure as hole transport material for efficient and stable inverted perovskite solar cells. Science China Chemistry, 2019, 62, 363-369.	4.2	36
49	Novel multi-color photoluminescence emission phosphors developed by layered gadolinium hydroxide via in situ intercalation with positively charged rare-earth complexes. Journal of Materials Chemistry C, 2015, 3, 1807-1816.	2.7	33
50	A peptide-based fluorescent chemosensor for measuring cadmium ions in aqueous solutions and live cells. Dalton Transactions, 2015, 44, 18057-18064.	1.6	33
51	Fabrication, gradient extraction and surface polarity-dependent photoluminescence of cow milk-derived carbon dots. RSC Advances, 2014, 4, 58084-58089.	1.7	31
52	Diammonium Porphyrin-Induced CsPbBr3 Nanocrystals to Stabilize Perovskite Films for Efficient and Stable Solar Cells. ACS Applied Materials & Interfaces, 2020, 12, 16236-16242.	4.0	31
53	Two-dimensional heterostructures built from ultrathin CeO <sub>2</sub> nanosheet surface-coordinated and confined metal–organic frameworks with enhanced stability and catalytic performance. Chemical Science, 2022, 13, 3035-3044.	3.7	30
54	Two-photon sensitized hollow Gd <sub>2</sub> O <sub>3</sub> :Eu <sup>3+</sup> nanocomposites for real-time dual-mode imaging and monitoring of anticancer drug release. Chemical Communications, 2016, 52, 1447-1450.	2.2	28

#	Article	IF	CITATIONS
55	Realizing high-performance lithium ion hybrid capacitor with a 3D MXene-carbon nanotube composite anode. Chemical Engineering Journal, 2022, 429, 132392.	6.6	28
56	A novel fluorescent chemosensor based on tetra-peptides for detecting zinc ions in aqueous solutions and live cells. Journal of Materials Chemistry B, 2016, 4, 4526-4533.	2.9	27
5 <b>7</b>	Hg2+-binding peptide decreases mercury ion accumulation in fish through a cell surface display system. Science of the Total Environment, 2019, 659, 540-547.	3.9	27
58	Eu <sup>2+</sup> /Eu <sup>3+</sup> -Based Smart Duplicate Responsive Stimuli and Time-gated Nanohybrid for Optical Recording and Encryption. ACS Applied Materials & Interfaces, 2019, 11, 1247-1253.	4.0	27
59	Dual-functional ratiometric fluorescent sensor based on mixed-lanthanide metal–organic frameworks for the detection of trace water and temperature. Inorganic Chemistry Frontiers, 2022, 9, 1406-1415.	3.0	27
60	Reducing methylmercury accumulation in fish using Escherichia coli with surface-displayed methylmercury-binding peptides. Journal of Hazardous Materials, 2019, 367, 35-42.	6.5	25
61	Perovskite surface management by thiol and amine copper porphyrin for stable and clean solar cells. Chemical Engineering Journal, 2021, 409, 128167.	6.6	25
62	AIE-based Tb3+ complex self-assembled nanoprobe for ratiometric fluorescence detection of anthrax spore biomarker in water solution and actual spore samples. Chemical Engineering Journal, 2021, 413, 127408.	6.6	25
63	Highly Controllable Hierarchically Porous Ag/Ag <sub>2</sub> S Heterostructure by Cation Exchange for Efficient Hydrogen Evolution. Small, 2021, 17, e2103064.	5.2	25
64	Mo <sub>2</sub> C-Ni-modified nitrogen-doped carbon nanofiber toward efficient hydrogen evolution reaction. New Journal of Chemistry, 2017, 41, 12956-12961.	1.4	24
65	A biomolecule-based fluorescence chemosensor for sequential detection of Ag+ and H2S in 100% aqueous solution and living cells. Sensors and Actuators B: Chemical, 2018, 273, 93-100.	4.0	24
66	Ultrafine MoP Nanoparticles Well Embedded in Carbon Nanosheets as Electrocatalyst with High Active Site Density for Hydrogen Evolution. ChemElectroChem, 2018, 5, 2256-2262.	1.7	23
67	Versatile rare-earth oxide nanocomposites: enhanced chemo/photothermal/photodynamic anticancer therapy and multimodal imaging. Journal of Materials Chemistry B, 2016, 4, 7832-7844.	2.9	22
68	A TAT peptide-based ratiometric two-photon fluorescent probe for detecting biothiols and sequentially distinguishing GSH in mitochondria. Talanta, 2020, 218, 121127.	2.9	22
69	Enhanced field emission performance of MXene–TiO <sub>2</sub> composite films. Nanoscale, 2021, 13, 7622-7629.	2.8	21
70	A reaction-and-assembly approach using monoamine zinc porphyrin for highly stable large-area perovskite solar cells. Science China Chemistry, 2020, 63, 777-784.	4.2	19
71	A nanocontainer that releases a fluorescence sensor for cadmium ions in water and its biological applications. Journal of Materials Chemistry, 2011, 21, 10298.	6.7	18
72	Core–Shell Lanthanide-Doped Nanoparticles@Eu-MOF Nanocomposites for Anticounterfeiting Applications. ACS Applied Nano Materials, 2022, 5, 1161-1168.	2.4	18

#	Article	IF	CITATIONS
73	An Elaborate Supramolecular Assembly for a Smart Nanodevice for Ratiometric Molecular Recognition and Logic Gates. Chemistry - A European Journal, 2016, 22, 8339-8345.	1.7	17
74	In Situ Growth of Ceria on Cerium–Nitrogen–Carbon as Promoter for Oxygen Evolution Reaction. Advanced Materials Interfaces, 2017, 4, 1700272.	1.9	17
75	Stimuliâ€Responsive Lanthanideâ€Based Smart Luminescent Materials for Optical Encoding and Bioâ€applications. ChemNanoMat, 2018, 4, 1097-1120.	1.5	17
76	A smart nanoprobe based on a gadolinium complex encapsulated by ZIF-8 with enhanced room temperature phosphorescence for synchronous oxygen sensing and photodynamic therapy. Dalton Transactions, 2019, 48, 16952-16960.	1.6	16
77	Tetraâ€ammonium Zinc Phthalocyanine to Construct a Graded 2D–3D Perovskite Interface for Efficient and Stable Solar Cells. Chinese Journal of Chemistry, 2019, 37, 30-34.	2.6	16
78	Self-assembly-induced luminescence of Eu3+-complexes and application in bioimaging. National Science Review, 2022, 9, nwab016.	4.6	16
79	Hierarchically porous MOF-based microneedles for glucose-responsive infected diabetic wound treatment. Materials Chemistry Frontiers, 2022, 6, 680-688.	3.2	16
80	Surface ligand coordination induced self-assembly of a nanohybrid for efficient photodynamic therapy and imaging. Inorganic Chemistry Frontiers, 2018, 5, 2620-2629.	3.0	14
81	Eu3+/Tb3+ supramolecular assembly hybrids for ultrasensitive and ratiometric detection of anthrax spore biomarker in water solution and actual spore samples. Talanta, 2021, 225, 122063.	2.9	14
82	Synthesis, Crystal Structures, and Luminescent Properties of Noninterpenetrating (6,3) Type Network Lanthanide Metal–Organic Frameworks Assembled by a New Semirigid Bridging Ligand. European Journal of Inorganic Chemistry, 2010, 2010, 5318-5325.	1.0	13
83	Smart nanoprobe based on two-photon sensitized terbium-carbon dots for dual-mode fluorescence thermometer and antibacterial. Chinese Chemical Letters, 2020, 31, 1792-1796.	4.8	13
84	4-Tert-butylpyridine-assisted low-cost and soluble copper phthalocyanine as dopant-free hole transport layer for efficient Pb- and Sn-based perovskite solar cells. Science China Chemistry, 2020, 63, 1053-1058.	4.2	13
85	Interesting Ag <sub>3</sub> PO <sub>4</sub> concave rhombic dodecahedra: the same face with different morphologies and photocatalytic properties. RSC Advances, 2017, 7, 23977-23981.	1.7	12
86	Octopus-Inspired Design of Apical NiS <sub>2</sub> Nanoparticles Supported on Hierarchical Carbon Composites as an Efficient Host for Lithium Sulfur Batteries with High Sulfur Loading. ACS Applied Materials & Interfaces, 2020, 12, 17528-17537.	4.0	12
87	Novel synthesis of <i>in situ</i> CeO <sub><i>x</i> </sub> nanoparticles decorated on CoP nanosheets for highly efficient electrocatalytic oxygen evolution. Inorganic Chemistry Frontiers, 2021, 8, 4440-4447.	3.0	12
88	Multiplex recognition and logic devices for molecular robot prototype based on an europium(iii)–cyclen system. Biosensors and Bioelectronics, 2018, 122, 1-7.	5.3	11
89	Intramolecular Electric Field Construction in Metal Phthalocyanine as Dopantâ€Free Hole Transporting Material for Stable Perovskite Solar Cells with >21 % Efficiency. Angewandte Chemie, 2021, 133, 6364-6369.	1.6	11
90	A Discrete 3d–4f Metallacage as an Efficient Catalytic Nanoreactor for a Three-Component Aza-Darzens Reaction. Inorganic Chemistry, 2022, 61, 4009-4017.	1.9	10

#	Article	IF	CITATIONS
91	A smart nanoprobe based on luminescent terbium metal–organic framework coated gold nanorods for monitoring and photo-stimulated combined thermal-chemotherapy. Journal of Rare Earths, 2022, 40, 1371-1381.	2.5	9
92	Synthesis and infrared and luminescence spectra of rare earth complexes with a new hexapodal ligand. Spectrochimica Acta - Part A: Molecular and Biomolecular Spectroscopy, 2006, 63, 164-168.	2.0	8
93	A smart tumor-microenvironment responsive nanoprobe for highly selective and efficient combination therapy. Inorganic Chemistry Frontiers, 2019, 6, 3562-3568.	3.0	8
94	Design of a versatile nanocomposite for †seeing' drug release and action behavior. Journal of Materials Chemistry B, 2015, 3, 8449-8458.	2.9	7
95	A Highly Selective and Sensitive Fluorescent Chemosensor for Aluminum Ions Based on Schiff Base. Journal of Fluorescence, 2016, 26, 2015-2021.	1.3	7
96	Assembly, crystal structure, and luminescent properties of three-dimensional (10,3)-a netted rare earth coordination polymers. Science in China Series B: Chemistry, 2008, 51, 614-622.	0.8	6
97	Synthesis, Crystal Structures and Luminescent Properties of Terbium, Neodymium and Yttrium Complexes with a New Amide Type Ligand. Zeitschrift Fur Anorganische Und Allgemeine Chemie, 2008, 634, 392-396.	0.6	6
98	Metalâ€Free Coupling of 3â€Alkenyl Oxoindoles by Nucleophilic Vinylic Substitution of Nitroolefins. Asian Journal of Organic Chemistry, 2013, 2, 307-310.	1.3	6
99	An Effective Strategy to Prepare Pd–Ag/MgCO3@α-Al2O3 Catalyst for Selective Hydrogenation of Acetylene. Catalysis Letters, 2017, 147, 483-490.	1.4	5
100	Activatable smart nanoprobe for sensitive endogenous MMP2 detection and fluorescence imaging-guided phototherapies. Inorganic Chemistry Frontiers, 2019, 6, 820-828.	3.0	5
101	Upconversion nanoparticles-labelled immunochromatographic assay for quantitative biosensing. New Journal of Chemistry, 2020, 44, 15498-15506.	1.4	5
102	Smart MMP2-Responsive Nanoprobe for Activatable Fluorescence Imaging-Guided Local Triple-Combination Therapies with Single Light. ACS Applied Bio Materials, 2019, 2, 2978-2987.	2.3	4
103	Synthesis, Crystal structure and Fluorescence properties of a Binuclear Terbium(lii) complex of N-(2-Pyridinyl)Ketoacetamide. Journal of Coordination Chemistry, 2004, 57, 257-264.	0.8	3
104	Synthesis and Luminescence Properties of Eu(III) and Tb(III) Complexes with Two New Amide Type Ligands. Synthesis and Reactivity in Inorganic, Metal Organic, and Nano Metal Chemistry, 2005, 35, 713-716.	0.6	3
105	Synthesis and Luminescence Properties of Rare Earth Complexes with Multipodal Ligands Containing Nâ€hydroxymethylsalicylamide. Synthesis and Reactivity in Inorganic, Metal Organic, and Nano Metal Chemistry, 2007, 37, 1-5.	0.6	3
106	Self-Assembly of Heterogeneous Structured Rare-Earth Nanocrystals Controlled by Selective Crystal Etching and Growth for Optical Encoding. ACS Applied Nano Materials, 2019, 2, 3518-3525.	2.4	3
107	A novel drug–drug nanohybrid for the self-delivery of porphyrin and <i>cis</i> -platinum. RSC Advances, 2019, 9, 37003-37008.	1.7	3
108	Dual-Functional Eu <sup>2+/3+</sup> -Complex@ZIF-67 Nanocatalyst Derived from a Green Reduction of Eu <sup>3+</sup> Compound. Inorganic Chemistry, 2020, 59, 13888-13897.	1.9	3

#	Article	IF	CITATIONS
109	Crystal Structure of the Lanthanum Nitrate Complex with N-(2-Amino-4-methylpyridinyl)benzoylacetamide. Analytical Sciences: X-ray Structure Analysis Online, 2007, 23, X71-X72.	0.1	2
110	Synthesis and Crystal Structure of 1,1'-Butane-1,4-diyl-dibenzimidazolium Picrate. X-ray Structure Analysis Online, 2009, 25, 31-32.	0.1	2
111	A two-dimensional lanthanide coordination framework with a new amide-type tripodal ligand,2,2′,2″-nitrilotris{[(2′-benzylaminoformyl)phenoxy]ethyl}amine. Chinese Journal of Chemistry, 2010, 22, 508-511.	2.6	2
112	A review of the studies on modern process for climatic proxies in north-western China. Frontiers of Earth Science, 2011, 5, 262.	0.9	2
113	Lanthanide-Functionalized Hydrophilic Magnetic Hybrid Nanoparticles: Assembly, Magnetic Behaviour, and Photophysical Properties. Nanoscale Research Letters, 2016, 11, 273.	3.1	2
114	Synthesis of Eu (III) and Tb (III) Complexes with Two New Amide Type Podands and Their Luminescence Properties. Chinese Journal of Chemistry, 2002, 20, 909-912.	2.6	1
115	Studies on metal charge density and band gap characteristics produced by the ( <sup>n</sup> BuCp) <sub>2</sub> ZrCl <sub>2</sub> compound and its reaction mechanism. RSC Advances, 2018, 8, 18406-18417.	1.7	1
116	Crystal Structure of 1,1'-Ethane-1,2-diyl-dibenzimidazolium Picrate. Analytical Sciences: X-ray Structure Analysis Online, 2007, 23, X73-X74.	0.1	0
117	Crystal Structure of the Erbium Nitrate Complex with N-(2-Pyridinyl)-ketoacetamide. Analytical Sciences: X-ray Structure Analysis Online, 2007, 23, X249-X250.	0.1	0
118	Crystal Structure of the Neodymium Picrate Complex with a Novel Amide Type Tripodal Ligand. Analytical Sciences: X-ray Structure Analysis Online, 2008, 24, X129-X130.	0.1	0
119	Factors Affecting Dehydrogenation and Catalytic Activity: Methyl Substituent. Catalysis Letters, 2018, 148, 2683-2695.	1.4	0
120	Frontispiece: Intramolecular Electric Field Construction in Metal Phthalocyanine as Dopantâ€Free Hole Transporting Material for Stable Perovskite Solar Cells with >21 % Efficiency. Angewandte Chemie - International Edition, 2021, 60, .	7.2	0
121	Frontispiz: Intramolecular Electric Field Construction in Metal Phthalocyanine as Dopantâ€Free Hole Transporting Material for Stable Perovskite Solar Cells with >21 % Efficiency. Angewandte Chemie, 2021, 133, .	1.6	0